

Supplementary Materials: Influence of Organic Ligands on the colloidal stability and removal of ZnO nanoparticles from synthetic waters by coagulation

Rizwan Khan ¹, Muhammad Ali Inam ¹, Du Ri Park ¹, Saba Zam Zam ¹, Sookyo Shin ¹, Sarfaraz Khan ², Muhammad Akram ³ and Ick Tae Yeom ^{1,*}

¹ Graduate School of Water Resources, Sungkyunkwan University (SKKU) 2066, Suwon 16419, Korea; rizwankhan@skku.edu (R.K.); aliinam@skku.edu (M.A.I.); enfl8709@skku.edu (D.R.P.); sabazamzam@skku.edu (S.Z.Z.); tkssk08@gmail.com (S.S.)

² Key Laboratory of the Three Gorges Reservoir Region Eco-Environment, State Ministry of Education, Chongqing University, Chongqing 400045, China; Sfk.jadoon@yahoo.com

³ Shandong Key Laboratory of Water Pollution Control and Resource Reuse, School of Environmental Science and Engineering, Shandong University, Qingdao 266200, China; m.akramsathio@mail.sdu.edu.cn

* Correspondence: yeom@skku.edu; Tel.: +82-31-299-6699

3. Results and discussion

3.1. ZnO NPs characterization

The Figure S1A shows the FT-IR spectra of ZnO NPs powder. The inset presents the same plot in the range from 2500 to 4000 cm^{-1} . The peak at 3650 cm^{-1} represents the OH stretching vibrations due to the physically absorbed water at the surface of particles. Moreover, some peaks in the region at 2896-2972 cm^{-1} corresponds to symmetric and asymmetric C-H stretching vibrations [1]. Moreover, the bands near 1377, 1150 and 1256 cm^{-1} were attributed to O-O, C-H, and C-O stretching vibrations and deformation of the CH_3 group respectively [2]. The peak at approximately 685 and 970 cm^{-1} corresponds to the stretching vibration of Al-C bond and Al-O stretching vibrations.

The X-ray diffraction (XRD) analysis of ZnO NPs was performed using X-ray diffractometer. The phase identification and percent (%) crystallinity were determined with the XRD pattern processing, identification, and quantification software (MDI Jade 7 v.7.5.11, Materials Data, Inc., Japan). The XRD pattern of the ZnO NPs is shown in (Figure S1B) with inset table showing following major peaks of (1 0 0), (0 0 2), (1 0 1), (1 0 2), (1 1 0), (1 0 3), (1 1 2) and (2 0 1). The sharp and narrow diffraction peaks indicated that the NPs powder is well crystalline. These reflections can be indexed to the known hexagonal crystal system wurtzite structure of ZnO NPs [3].

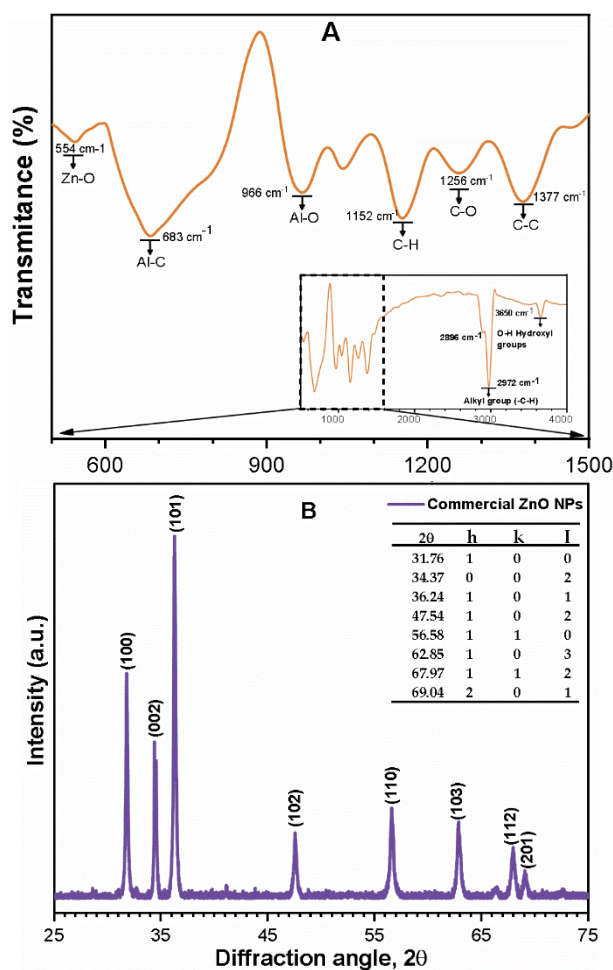


Figure S1. (A) FT-IR spectra and ;(B) XRD pattern of commercial ZnO NPs powder.

Table S1. ZnO NPs physicochemical properties.

Parameter	Unit	Technique	Value
Vendor-reported primary size	nm	TEM	<50
Density	$\text{g}(\text{cm}^3)^{-1}$	-	5.60
BET specific surface area	m^2g^{-1}	BET	12.2±0.4
Isoelectric point (IEP, see Fig 1B)	-	Zetasizer	9.2
Zeta potential in pure water (pH=7)	mV	Zetasizer	+14±2.1
HDD measured in pure water	nm	DLS	280±35
Purity / moisture content	wt.%	TGA / ICP-OES	97.27 / 1.61
phase and structure (Figure 1B)	-	XRD	100% hexagonal
Hamaker Constant	$\text{J}^{(a)}$	-	1.9×10^{-20}
Net energy barrier in pure water (IS 5×10^{-6} M)	$\text{kT}^{(b)}$	-	42.8

(a) [4], (b) $1 \text{ kT} = 4.1142 \times 10^{-21} \text{ J}$ at $25 \pm 1^\circ\text{C}$

3.1.2. Determination of wavelength through UV-vis spectrophotometer

The concentration-absorption relationship of ZnO NPs within a specific range can obey the Beers-Lambert law, thus the change of UV absorbance may reflect the individual ZnO NPs concentration [5]. As shown (Fig S1 C.) in the full wavelength scanning (200–800 nm), data spectrum of (0–50mg/L) ZnO NPs show a broad peak at λ 370 nm. Moreover, it can be observed that the absorbance intensity of peak varies with the concentration throughout the wavelength range of 200 to 800 nm. Based on this, 370 nm wavelength was chosen for absorbance measurement of ZnO NPs during the aggregation experiment.

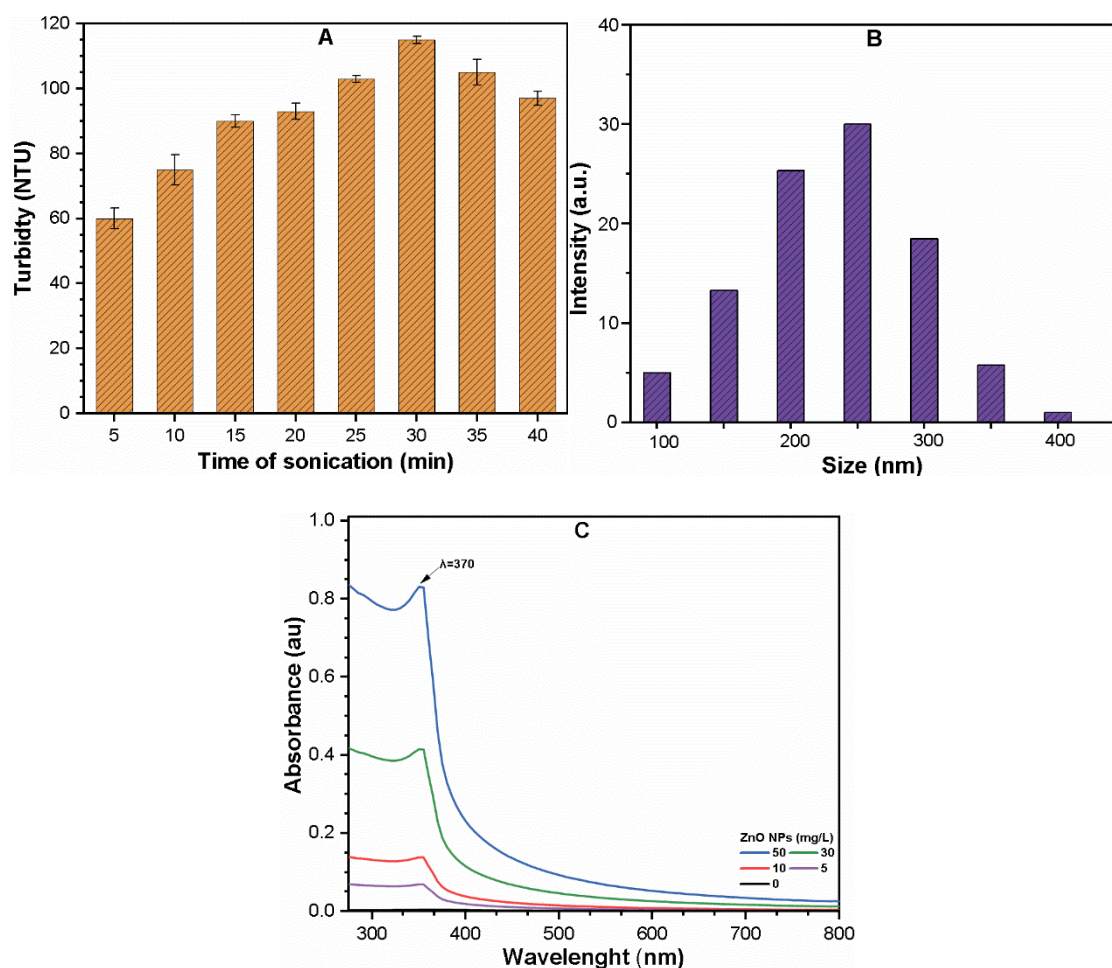


Figure S2. (A) Effects of sonication time (5–40 min) on the dispersion turbidity of (30 mg/L) ZnO NPs; (B) Hydrodynamic size distribution of ZnO NPs in water after 30 min sonication; (C) UV-Vis spectra of ZnO NPs at a various initial concentration (0–50 mg/L).

Table S2. The Relative concentration of C, N, H and S in various organic ligands.

Ligand type	C %	H%	N%	S %	C/N Ratio	C/H Ratio
Humic acid	61.29	4.52	1.32	0.63	46.43	13.55
Salicylic acid	35.40	3.65	0.98	0.49	36.12	9.69
L-cysteine	27.63	5.45	7.59	24.68	3.64	5.06

3.2. Adsorption Kinetics of Organic Ligands

The adsorption kinetics of HA, SA, and L-cys onto the ZnO NPs surface were fitted with two commonly used Lagergren pseudo-first order (PFO) and Ho pseudo-second-order (PSO) models as shown linear form equation 1 and 2 respectively.

$$\log(q_e - q_t) = \log q_e - \frac{k_1 t}{2.303} \quad (1)$$

$$\frac{t}{q_t} = \frac{1}{k_2 q_e^2} + \frac{t}{q_e} \quad (2)$$

Where: q_e and q_t are the amounts of ligands adsorbed (mg/g) at equilibrium and at time t (h), respectively. k_1 and k_2 are rate constants adsorption (h⁻¹) of PFO and PSO models, respectively.

Table S3. The pseudo-second-order (PSO) model parameters used to describe adsorption of HA, SA, and L-cys on ZnO NPs.

Adsorbate	q_e (mg/g)	k (g/mg/h)	v_0 (mg/g/h) ^a	Adj.R ²
HA	41.78	0.138	240.89	0.976
SA	10.44	0.0632	6.87	0.972
LC	21.52	0.0681	31.53	0.986

^a adsorption rate (v_0) was calculated with $v_0 = kq_e^2$.

Table S4. The Dissolution of ZnO NPs and the change of suspension pH in synthetic waters.

		Synthetic waters							
Measurement	Milli-Q Water	S1	S2	S3	S4	S5	S6	S7	S8
Suspension pH after 24h	7.01 ± 0.10	7.18 ± 0.07	7.25 ± 0.12	6.98 ± 0.11	7.12 ± 0.06	6.85 ± 0.07	6.95 ± 0.04	6.75 ± 0.18	6.70 ± 0.09
Dissolved Zn ²⁺ mg L ⁻¹ After 24h	0.91 ± 0.023	0.24 ± 0.013	0.15 ± 0.010	0.91 ± 0.022	1.21 ± 0.015	1.66 ± 0.018	1.38 ± 0.054	2.26 ± 0.015	2.54 ± 0.020

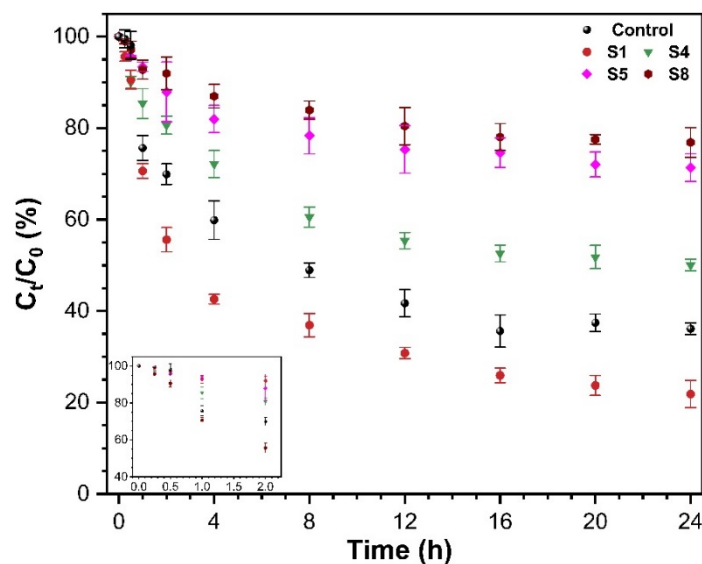


Figure S3. Aggregation of ZnO NPs (10mg/L) in selected synthetic waters.

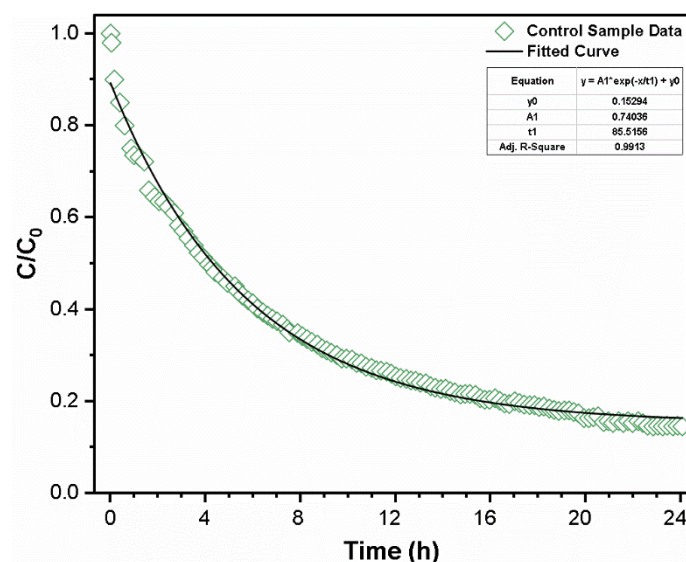


Figure S4. The fit of aggregation data to the Stokes' equation. Exponential model for ZnO NPs (30 mg/L), at pH 7 in nanopure water.

References

1. Matrajt, G.; Borg, J.; Raynal, P. I.; Djouadi, Z.; d'Hendecourt, L.; Flynn, G.; Deboffe, D. FTIR and Raman analyses of the Tagish Lake meteorite: Relationship with the aliphatic hydrocarbons observed in the Diffuse Interstellar Medium. *Astron. Astrophys.* **2004**, *416*, 983–990.
2. Vlachos, N.; Skopelitis, Y.; Psaroudaki, M.; Konstantinidou, V.; Chatzilazarou, A.; Tegou, E. Applications of Fourier transform-infrared spectroscopy to edible oils. *Anal. Chim. Acta* **2006**, *573–574*, 459–465, doi:10.1016/j.aca.2006.05.034.
3. Selvarajan, E.; Mohanasrinivasan, V. Biosynthesis and characterization of ZnO nanoparticles using *Lactobacillus plantarum* VITES07. *Mater. Lett.* **2013**, *112*, 180–182.
4. Ackler, H. D.; French, R. H.; Chiang, Y.-M. Comparisons of Hamaker constants for ceramic systems with intervening vacuum or water: From force laws and physical properties. *J. Colloid Interface Sci.* **1996**, *179*, 460–469.
5. Kristiansson, O.; Lindgren, J.; De Villepin, J. A quantitative infrared spectroscopic method for the study of the hydration of ions in aqueous solutions. *J. Phys. Chem.* **1988**, *92*, 2680–2685, doi:10.1021/j100320a055.